Advances in
Bridge Engineering

ORIGINAL INNOVATION Open Access

Numerical modeling of hydrodynamic added mass and added damping for elastic bridge pier

Yanfeng Wang[1] and Zilong Ti[1*]

*Correspondence:
zilongti@swjtu.edu.cn

[1] State Key Laboratory of Bridge Intelligent and Green Construction, Southwest Jiaotong University, Chengdu, Sichuan 611756, China

Abstract

This paper presents a numerical model using the boundary element method for determining the hydrodynamic added mass and added damping of an elastic bridge pier with arbitrary cross-section. Combining the Euler–Bernoulli beam theory with the constant boundary element method, the modal superposition method is used to consider the deformable boundary conditions on the surface of elastic piers to couple the interaction between the elastic pier and water, and the equations for the hydrodynamic added mass and added damping of a general section pier considering the effect of pier-water coupling are derived. The accuracy of the developed model is verified by a benchmark experiment. The developed model is calculated for circular piers and compared with the added mass analytical formulation. The effects of oscillating frequency and structure geometry on the added mass and added damping are further investigated. Results demonstrate that the developed model can be used to solve the hydrodynamic added mass and added damping problems of the elastic bridge pier. Compared to the analytical formula, the developed method incorporates the consideration of added damping in the analysis of the pier-water coupling problem. Oscillating frequency and structure geometry have significant effects on added mass and added damping.

Keywords: Sea-crossing bridge, Elastic piers, Hydrodynamic, Added mass, Added damping, Boundary element method

1 Introduction

The construction of sea-crossing bridges has experienced rapid advancement to enhance the transportation among islands and regions in the global coastal community, such as the Hong Kong-Zhuhai-Macau Bridge (Li and Chen 2011), Hangzhou Bay Cross-Sea Bridge (Lu 2006), Qingdao Bay Bridge (Dong and Jin 2009), etc. The piers of sea-crossing bridges are immersed in water and subjected to harsh wave effects (Liu 2019; Ti et al. 2020c; Wei et al. 2020; Yang et al. 2021). Previous studies confirm that the energy of waves is primarily concentrated in the low-frequency range between 0 and 0.5 Hz

(Murray and Rastegar 2009; Guo et al. 2016). Long-span bridges built in coastal areas have minor fundamental frequencies and are easily coupled with waves to produce unfavorable dynamic effects, and thus it is important to examine the coupling issue between water and elastic piers (Ti et al. 2020b; Chen et al. 2021; Zhao et al. 2022). When a structure is submerged or partially submerged in water, the relative motion between them generates additional hydrodynamic forces on the structure. It may obviously alter the fundamental characteristics of the structure and the resultant dynamic responses. Therefore, it is necessary to accurately estimate such a coupling process associated with the added hydrodynamic forces.

The additional hydrodynamic force is often considered as the combination of added mass and damping to reduce the complexity and simplify the calculation (Yeung 1981; Rahman and Bhatta 1993; Kristiansen and Egeland 2003). The added mass represents the effective mass of water that participates in the structural vibration through the fluid–structure coupling. The initial proposal of this concept can be attributed to Westergaard (1933), who examined the hydrodynamic pressure analysis of rigid dams subjected to harmonic ground motion. Several scholars have employed analytical methods to investigate the coupling between fluid and structure. For example, Liaw and Chopra (1974) introduced an analytical formulation grounded in radiation theory to derive an equation representing the added mass for circular columns immersed in water. Under the presumption of uniform distribution of added mass over the water depth, Han (1996) formulated an added mass equation for elastic structures by utilizing the first-order frequency reduction rate. Due to the complexity of solving the added mass analytical equation, Li and Yang (2013) and Jiang et al. (2017) proposed a simplified equation by fitting the data to the added mass analytical equation for the cylinder. Besides the circular cross-section, Yang and Li (2012) and Wang et al. (Wang et al. 2018a; b) proposed simplified formulae for the added mass of square, rectangular, elliptical, and circular end forms before and after. All of the aforementioned research disregarded the impact of free surface waves and did not take added damping into account. Some scholars have specifically studied the effect of free surface waves on hydrodynamic pressure. Huang and Li (2011) noted that the influence of the free surface wave on the hydrodynamic pressure is significant primarily at low frequencies of the applied load excitation. By using boundary conditions with or without taking into account the free surface wave, Xing et al. (1997) examined the horizontal motion of an elastic cylinder parallel to the water's surface and concluded that the free surface wave has a significant impact on the vibration characteristics of the structure with low frequency coupling effects. The presence of surface waves on the liquid surface impedes the motion of the structure and generates an additional damping force (Romate 1992; Kim et al. 1997; Perić and Abdel-Maksoud 2016). Therefore, it is important to consider the influence of added damping when studying the coupling effects between water and elastic structures.

The aforementioned solutions for added mass and added damping primarily rely on analytical methods, which are straightforward to apply but only limited to columns with uniform cross-sections. Advanced numerical approaches have the capability to simulate complex coupling interactions between fluids and arbitrary geometric structures. Zhang et al. (2019) developed a potential-based numerical model using ADINA to calculate the added mass of submerged column with arbitrary cross-section under

seismic action. Computational fluid dynamics (CFD) is one of the popular numerical methods for analyzing the fluid–structure coupling effect (Huang et al. 2009, 2018; Xu and Cai 2015; Ti et al. 2020a). CFD can comprehensively capture fluid motion for the evaluation of wave load, but it is associated with drawbacks such as high computational cost and a large amount of data. Fortunately, the boundary element method (BEM) based on potential flow theory can discretize the body surface into a finite number of panels and establish the integral equation to solve fluid–structure coupling issues by integrating over the object surface, which can efficiently and quickly evaluate the hydrodynamic loads of offshore structures, ships, bridge piers, etc. (Teng and Taylor 1995; Choi et al. 2001; Chen and Mei 2016; Ti et al. 2019). For example, Teng and Gou (2006) employed the high-order boundary element method to compute the interaction between waves and large elastic floating bodies. Shen et al. (2012) proposed a numerical model that combines the boundary element method and high-order finite element method to study the interaction between waves and elastic plates. Ti et al. (2020b) proposed a numerical model based on the boundary element method to solve the coupled response of elastic structures and waves. Since the added mass and added damping are the effective methods to characterize the structural hydrodynamic force, the numerical model to evaluate the added mass and added damping of elastic bridge piers with the aid of the boundary element method can be a reference for the basic design and research of sea-crossing bridges.

In this paper, a numerical approach is presented for solving the general hydrodynamic added mass and added damping of the elastic piers with arbitrary cross-section considering the effect of pier-water coupling by combining the Euler–Bernoulli beam theory with the boundary element method and basing on the potential flow theory. Firstly, the effectiveness of the developed method was verified by a benchmark experiment. Then added mass of the circular section bridge pier is calculated using the presented model and compared with conventional analytical methods. The effects on the wet period and wet damping ratio of the structure are clarified. The influence of oscillating frequency and geometry on the added mass and added damping is discussed as well.

2 Numerical model and validation

2.1 The process of pier-water coupling

The fundamentals of dynamic coupling between elastic structures and fluids encompasses two main aspects: hydrodynamics and structural dynamics. When the elastic pier-water coupling system oscillates at a frequency of ω under steady-state conditions, based on potential flow theory, the velocity potential can be expressed as follows:

$$\Phi(x, y, z, t) = a\phi_r(x, y, z)e^{-i\omega t} \tag{1}$$

where: $\phi_r(x, y, z)$ represents the spatial component of the radiation velocity potential and a denotes the amplitude of the velocity potential under the harmonic excitation. The velocity potential should satisfy the Laplace's equation and boundary conditions, which include the free surface boundary condition, seabed boundary condition, and

far-field boundary condition. The detailed formulations for each boundary condition are described in the literature (Ti et al. 2022) and not listed here for the sake of conciseness.

The radiation potential satisfies:

$$\frac{\partial \phi_r}{\partial n} = v(x, y, z) \tag{2}$$

where n is the normal vector and $v(x, y, z)$ is the velocity amplitude of the structure's motion. Using the modal superposition principle in structural dynamics, the structural displacement $u(x, y, z)$ can be expressed in the form of a sum of individual modes:

$$v(x, y, z) = -i\omega u(x, y, z) = \sum_{j=1}^{m} -i\omega \varphi_j(x, y, z)\xi_j \tag{3}$$

where m is the number of modes, $\varphi_j(x, y, z)$ is the j_{th} mode, and ξ_j is the j_{th} mode coordinate. Correspondingly, the radiation potential ϕ_r can be expressed as:

$$\phi_r = -i\omega \sum_{j=1}^{m} \xi_j \phi_{r,j} \tag{4}$$

where $\phi_{r,j}$ is the radiation potential induced when the pier vibrates with the unit amplitude of the j_{th} mode. Equation (4) realizes the pier-water coupling, and the coupling process is shown in Fig. 1.

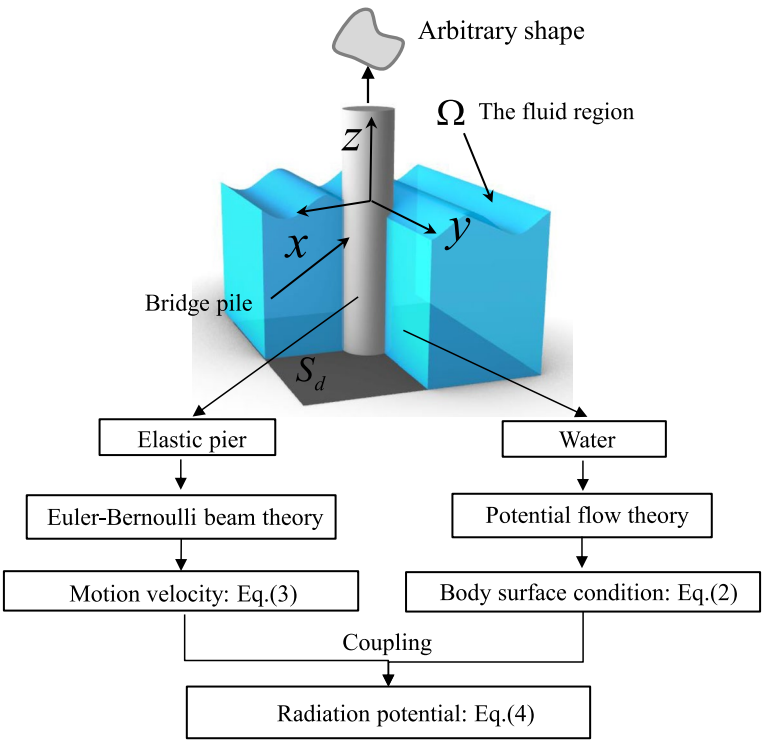

Fig. 1 Flowchart of analysis framework for the pier-water coupling process

Figure 1 shows an elastic pier with a fixed bottom and arbitrarily shaped cross-section surrounded by water, where S_d denotes the seafloor, $Oxyz$ is the right-handed coordinate system, and $z = 0$ indicates the average free surface.

By using the linear Bernoulli equation, the dynamic pressure can be obtained as:

$$p = -\rho \frac{\partial \phi}{\partial t} = i\omega\rho(\phi_i + \phi_d) + \omega^2 \sum_{j=1}^{m} \xi_j \phi_{r,j} \tag{5}$$

where ρ is the density of fluid.

The solution of hydrodynamic pressure is crucial in analyzing pier-water coupling problems. Traditional analytical methods encounter challenges when solving the coupling problem between bridge piers with complex cross-sections and fluid. However, the boundary element method offers a practical numerical approach by discretizing the surface of the structure into a finite number of panels. This facilitates the solution of the pier-water coupling problem for geometrically diverse cross-sections. Using the second Green's theorem, the boundary integral issue for the constant boundary element is as follows:

$$\alpha\phi(x_0, y_0, z_0) = \iint_S \frac{\partial \phi(x, y, z)}{\partial n} G(x, y, z; x_0, y_0, z_0) ds - \iint_S \frac{\partial G(x, y, z; x_0, y_0, z_0)}{\partial n} \phi(x, y, z) ds \tag{6}$$

where x_0 is the source point, α is the solid angle coefficient, $\alpha = 1$ indicates the source point is in the fluid region, and $\alpha = 1/2$ denotes the source point is on the body surface. The free-surface Green's function G proposed by John (1949; John 1950) is utilized in this paper.

2.2 Hydrodynamic added mass and added damping

By integrating the body surface pressure along the length of the beam element, the equivalent hydrodynamic force at each node of the beam can be obtained:

$$\mathbf{f} = \int_{S_e} p\, \mathbf{N}^T dS = \mathbf{f}_i + \mathbf{f}_d + \mathbf{f}_\mathbf{r} \tag{7}$$

where $\mathbf{N}$ is the shape function matrix, $\mathbf{f}_i$, $\mathbf{f}_d$ and $\mathbf{f}_r$ are respectively the equal effectiveness vectors of the incident, diffraction and radiation waves, and S_e represents the wetted surface of the structure. By substituting Eq. (5) into Eq. (7), the radiation force can be expressed as follows:

$$\mathbf{f}_r = \sum_{j=1}^{m} (\omega^2 \mathbf{m}_{w,j} + \mathrm{i}\omega \mathbf{c}_{w,j}) \xi_j \tag{8}$$

where $\mathbf{m}_w$ and $\mathbf{c}_w$ are the added mass and the added damping of the element.

$$\mathbf{m}_w = \mathrm{Re}[\rho \int_{S_e} \phi_{r,j} \mathbf{N}^T dS] \tag{9}$$

$$\mathbf{c}_w = \mathrm{Im}[\omega\rho \int_{S_e} \phi_{r,j}\mathbf{N}^T dS] \tag{10}$$

The dynamic equation of the structure considering the pier-water coupling effect is given by:

$$\sum_{j=1}^{m} [-\omega^2(\mathbf{M}\varphi_j + \mathbf{M}_{w,j}) - \mathrm{i}\omega(\mathbf{C}\varphi_j + \mathbf{C}_{w,j}) + \mathbf{K}\varphi_j]\xi_j = \mathbf{F_{ex}} \tag{11}$$

where $\mathbf{M}$, $\mathbf{K}$ and $\mathbf{C}$ correspond to the structure's global mass matrix, stiffness matrix, and damping matrix, respectively. $\mathbf{F_{ex}}$ is the exciting force, $\mathbf{M}_w = \mathbf{m}_w\varphi$, $\mathbf{C}_w = \mathbf{c}_w\varphi$. It should be noted that the added mass discussed below is $\mathbf{M}_w$, and the added damping is $\mathbf{C}_w$. The modal amplitude ξ_j is the only unknown quantity in the above equation, which can be obtained by solving linear equations.

2.3 Fundamental period and damping ratio

The added mass and added damping cause the structural dynamic properties to change. In the following analysis, the iterative method is employed to investigate the influence of added mass and added damping on the fundamental period and damping ratio of the structure. The first-order mode is considered as an example for this study. First, using $\omega_{1,s}$ and $\varphi_{1,s}$ of the structure in the first mode of free vibration in the air, the corresponding radiation potential $\phi_{r,1}$ is obtained for $\mathbf{M}_w$ and $\mathbf{C}_w$. Then the frequencies $\omega_{1,w}$ and modes $\varphi_{1,w}$ of vibration in water are calculated by substituting $\mathbf{M}_w$ and $\mathbf{C}_w$ into the eigenvalue equation and repeating the above steps to obtain the

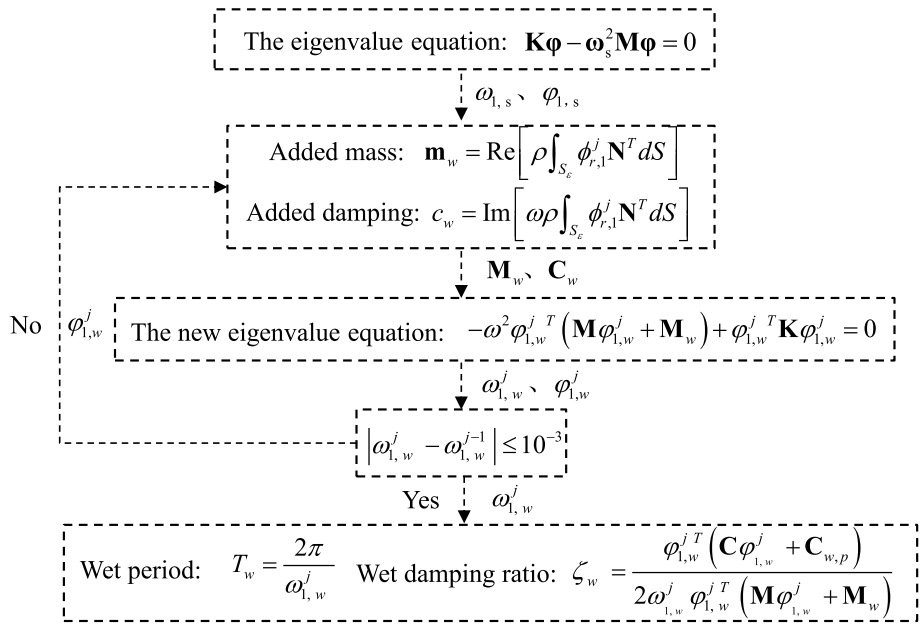

Fig. 2 Flowchart to investigate fundamental period and damping ratio considering the pier-water coupling effect

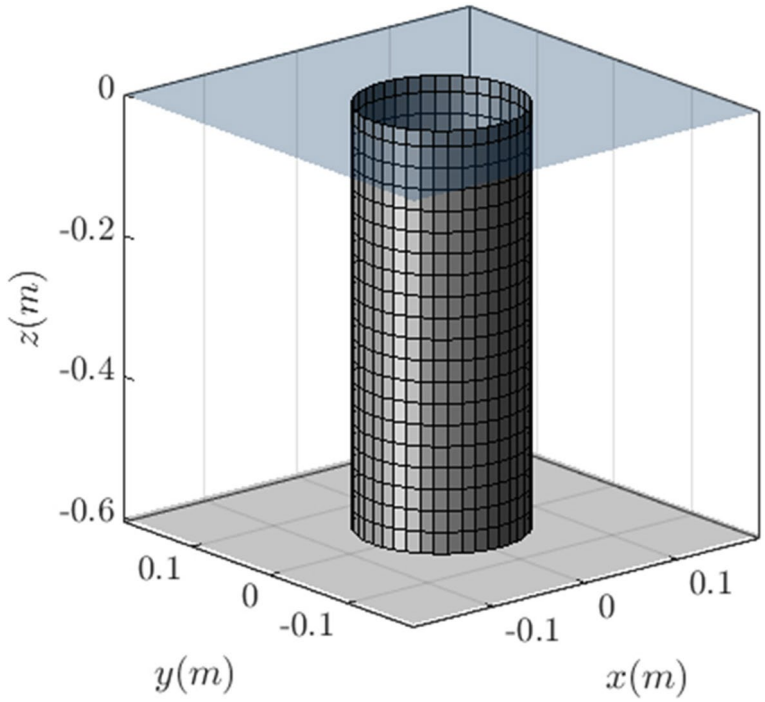

Fig. 3 Discretized panels of the experimental model

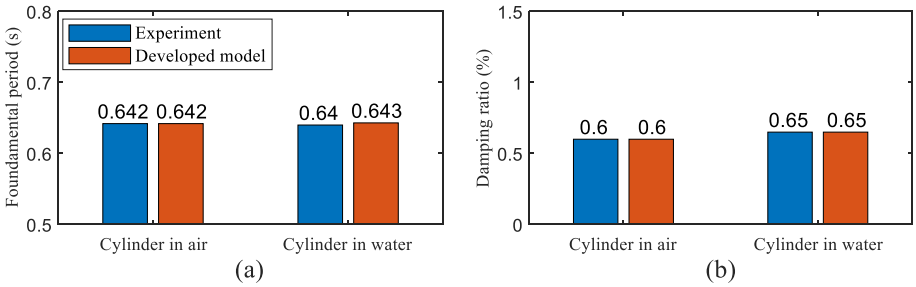

Fig. 4 Developed and experimental results of fundamental period and damping ratio for benchmark model: **a** fundamental period; and **b** damping ratio

correlative $\phi_{r,1}^2$, $\mathbf{M}_w$ and $\mathbf{C}_w$. Repeatedly iterating j times until the frequency $\left|\omega_{1,w}^{j} - \omega_{1,w}^{j-1}\right| \leqslant 10^{-3}$ obtained before and after two times, the period and damping ratio after considering the fluid–structure coupling effect can be obtained by $\omega_{1,w}^{j}$. The specific iterative process is shown in Fig. 2.

2.4 Experimental validation

The benchmark experiment reported in the literature (Bai 2018) investigated the dynamic fluid–structure coupling issue of an elastic cylinder fixed at the bottom under wave action. The specific experiment model and wave parameters are detailed in the literature (Bai 2018). To determine the validity of the code, the experimental model is replicated and calculated using the developed method and compared with the test results. The water depth is 0.6 m. The numerical model is constructed using

the developed method, with the structural bottom fully constrained. The structural submerged part is discretized into 800 quadrilateral panels, as shown in Fig. 3.

The fundamental periods and damping ratios of the model's vibration are tested separately in air and water, representing the conditions without and with the presence of water, respectively. The results depicted in Fig. 4 demonstrate an increase in both the fundamental period and damping ratio in the presence of water. Moreover, the increase in the damping ratio is more pronounced, indicating that water has a greater impact on the damping characteristics. The calculated results are in good agreement with the experimental results. This demonstrates that the developed method provides a reasonably accurate estimation of the structural characteristics when considering the coupling effect between the elastic structure and water. It also reflects the high precision of the proposed method in solving the added mass and added damping.

3 Case study and discussions

Previous analytical methods often simplify the calculation by treating the structure as a rigid body and neglecting the influence of the free water surface. However, it is necessary to investigate the impact of structural elasticity and the free water surface on the added mass and added damping. Furthermore, the discrepancies in added mass and added damping among different cross-sections require further examination. This paper utilizes a circular cross-section pier with analytical solutions for hydrodynamic coefficients as the fundamental model case. As shown in Fig. 5, the bottom of the circular pier is fastened to the seafloor, with a diameter of 12 m and a height of 100 m. The equivalent stiffness is 15,800 GN·m^2, and the mass is 84.7 kN/m. The wave amplitude A is 1 m, the water depth is 90 m, and the fluid density ρ_w is 1000 kg/m^3. A concentrated mass is added at the free end of the pier top to simulate the effect of the bridge superstructure mass. The fundamental frequency of the circular pier is 0.236 Hz and the damping ratio is 0.05.

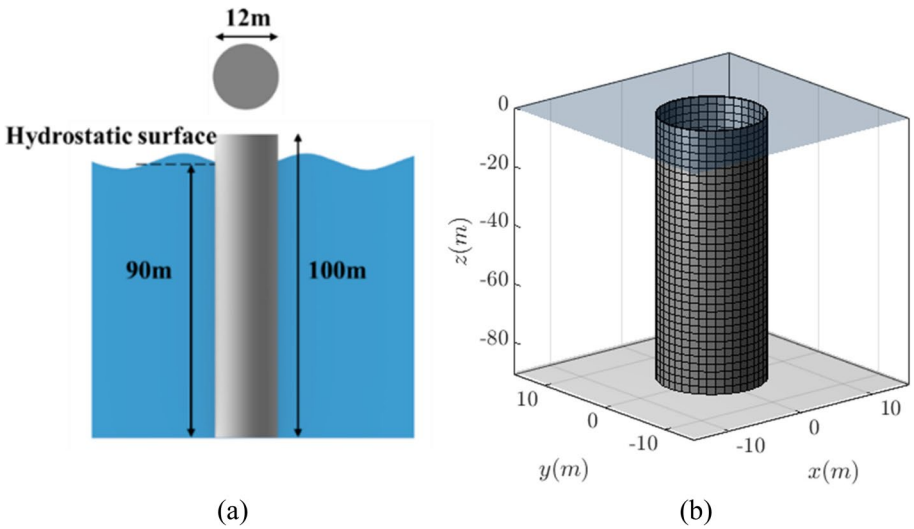

Fig. 5 Dimensions and panel discretization of the studying circular pier: **a** dimensions of the case pier; and **b** discretized panels on the submerged surface

3.1 Comparison with analytical formula

The added mass formula proposed by Liaw and Chopra (1974) based on radiation wave theory is widely cited in engineering. It is elected to calculate the added mass of the circular pier model and compared with the developed method.

Equation from Liaw and Chopra (1974):

$$m_a{}'(z') = 4\rho_w \pi D \sum_{1}^{N_q} \frac{I_q}{2\lambda'_q H_w} E_q\left(\frac{\lambda'_q D}{2}\right) \cos\left(\alpha_q z'\right) \tag{12}$$

where D is the diameter, H_w is the water depth, z' is the location along the height of the circular pier, the bottom of the pier $z' = 0$, $I_q = \int_0^{H_w} \cos\left(\alpha_q z'\right) dz'$, $\lambda'_q = \alpha_q = (2q-1)\pi/2H_w$, $E_q(x) = K_1(x)/(K_0(x) + K_2(x))$, $K_n(x)$ is the modified Bessel function of order n of the second kind, $q = 1, 2, ..., N_q$, where N_q is the number of terms, take the number of terms greater than 50 has better convergence, and this paper is taken as 60. Since Liaw and Chopra (1974) ignores the effect of added damping, the following discussion ignores it.

Using the developed method and the formulas from Liaw and Chopra (1974), the added mass and added damping distribution per unit length of the circular pier are computed when it undergoes free vibration at the first-order mode. It should be emphasized that the computation of the added mass and added damping presented in this study is based on the normalization of the first-order mode. The corresponding results are depicted in Fig. 6. Where $z/h_w = 0$ denotes the water surface and $z/h_w = -1$ denotes the pier bottom.

The results show that the added masses calculated by both methods have the same overall trend along the pier height, which grows rapidly from the free surface to $z = 0.2h_w$ and then decreases gradually with increasing water depth. It is found that the added mass calculated by Eq. (12) considering the structure as a rigid body is larger than that calculated by accounting for the elasticity of the structure, which is also mentioned in Liaw and Chopra (1974). The analytical formulation ignores the free surface waves, which leads to disregarding the effect of added damping. However,

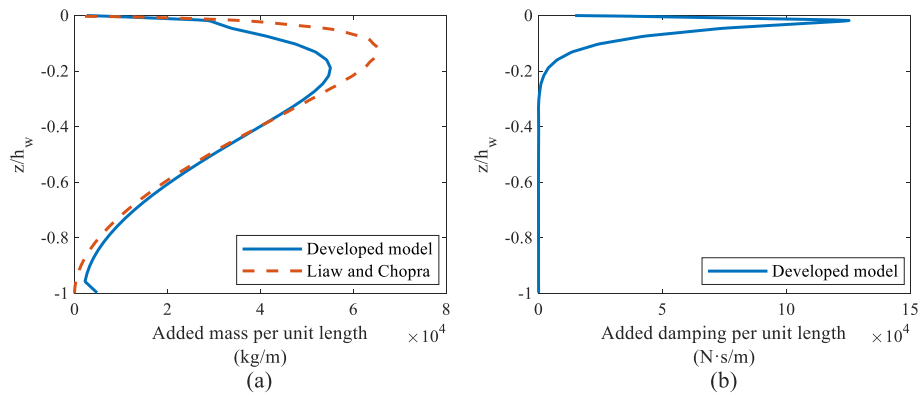

Fig. 6 Comparison of the distribution of added mass and added damping along the height of the bridge pier between results from Liaw and Chopra (1974) and developed model: **a** Added mass; and **b** Added damping

it is evident from Fig. 6 that the added damping exhibits a similar magnitude as the peak added mass. The added damping is larger near the water surface, indicating that the influence of the surface waves is critical.

Considering added mass and added damping change the fundamental period and damping ratio of the structure. To assess the effect of calculated results from the above two methods on these structural properties, a comparison is made against the characteristics of the original structure unaffected by hydrodynamic effects, as shown in Fig. 7. The developed method demonstrated a 2.6% increment in the fundamental period and a notable 14.4% rise in the damping ratio when compared to the characteristics of the original structure. The data indicates that the influence of added damping on structural damping ratio is quite significant. Therefore, when analyzing the coupling between elastic piers and water, it is essential to consider the effects of added damping. In contrast, the fundamental period computed using the result from Liaw and Chopra (1974) experienced a 3.8% increase. Since the analytical formula does not consider added damping, the damping ratio does not change.

3.2 Effect of oscillating frequency

The developed method takes into account the influence of the free surface wave, and the boundary condition for the free water surface is expressed as follows:

$$\frac{\partial \phi(x,y,z)}{\partial z} = \frac{\omega^2}{g}\phi(x,y,z) \tag{13}$$

where $g = 9.81\text{m/s}^2$. From Eqs. (4), (9), (10), and (13), it is evident that the added mass and added damping are related to the structural oscillating frequency, taking into account the influence of free surface waves. In order to investigate the influence of oscillating frequency on the added mass and added damping, this section presents the computation of the added mass and added damping of the circular pier under the harmonic

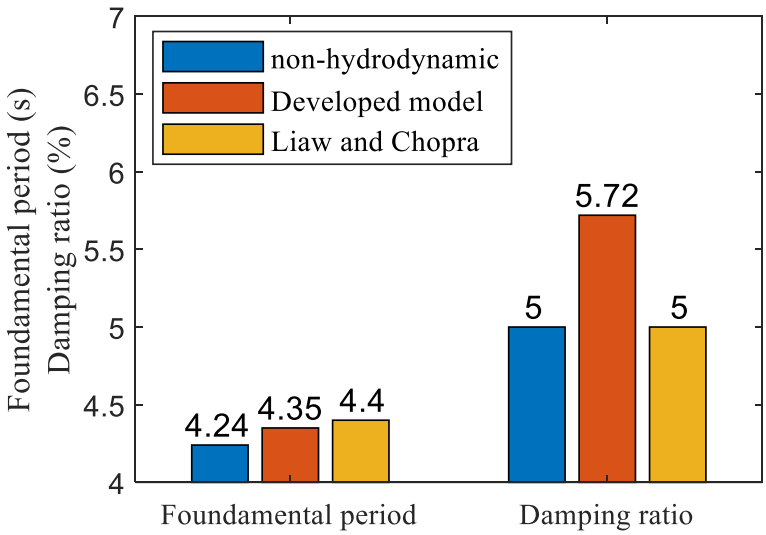

Fig. 7 Comparison of fundamental period and damping ratio between results from Liaw and Chopra (1974), developed model, and case without hydrodynamic effect

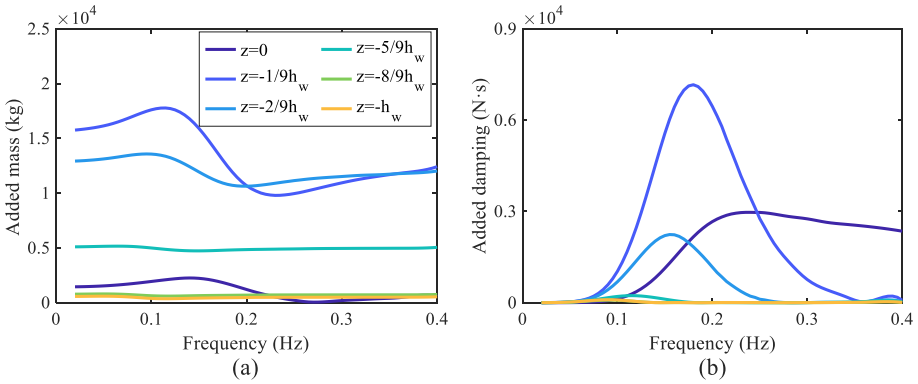

Fig. 8 Distribution of added mass and added damping with oscillating frequency at different locations: **a** Added mass; and **b** Added damping

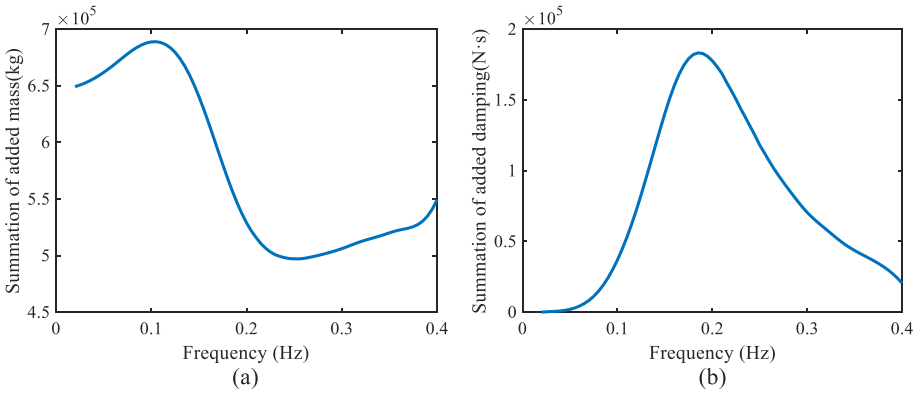

Fig. 9 Distribution of total added mass and total added damping with oscillating frequency: **a** Added mass; and **b** Added damping

excitation with unit wave amplitude within the frequency range of 0.02 Hz to 0.4 Hz. To gain a deeper understanding of the distribution of added mass and added damping along the height of the pier, six specific positions are chosen for calculation. Furthermore, through the integration of the added mass and damping values along the water depth, the total added mass and added damping can be obtained for various oscillating frequencies. The results are shown in Figs. 8 and 9. Where z is the location along the pier height and h_w represents the water depth, $z = 0$ represents the location on the surface and $z < 0$ represents the submerged location.

As shown in Fig. 8, the oscillating frequency exerts varying degrees of influence on the added mass and added damping at different heights, indicating the significance of considering the surface wave effects induced by radiation. In particular, the impact is most significant from the water surface to $z = -2/9h_w$, while it is less prominent near the bottom of the pier. This is attributed to the strong surface wave effects near the water surface, whereas the dynamic water pressure induced by surface waves diminishes with increasing water depth.

Figure 9 shows the strong frequency dependence of the total added mass and the total added damping. The sum of the added mass peaks at a frequency close to 0.1 Hz. One probable explanation is that the harmonic excitation force at 0.1 Hz is powerful

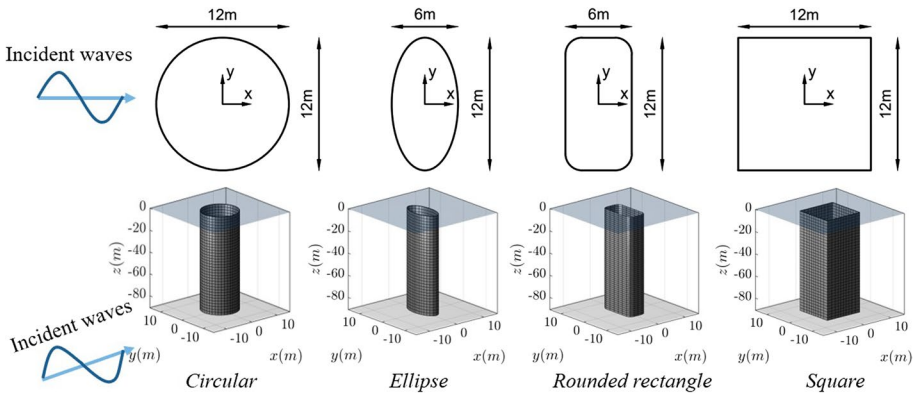

Fig. 10 Dimensions and discretized meshes of different cross-sections

and accelerates the motion of the structure. This leads to a greater involvement of water mass in the structural motion, resulting in a significant increase in inertial mass. And the sum of added damping peaks at the oscillating frequency near the fundamental frequency. The reason could be attributed to the resonance of the structure, which causes the surrounding water to vibrate together. This phenomenon results in the continuous dissipation of the structural kinetic energy and a prominent value of added damping.

To sum up, the added mass and added damping are sensitive to the oscillating frequency and have different peak frequencies. Furthermore, the distribution of added mass and added damping is primarily concentrated from the water surface to $z = -2/9h_w$.

3.3 Effect of geometry

Geometry has a significant influence on the pier-water interaction. In order to investigate the effect of geometry on added mass and added damping, four cross-sections commonly used for bridge piers, i.e., circular, elliptical, rounded rectangular and square are selected to compare to find a cross-section that may be most suitable relative to the pier-water coupling problem. Note that geometric properties such as length, water depth, area, density, mass, and stiffness are kept consistent with the previous circular pier case to exclusively study the effect of cross-sectional geometry. To ensure consistent obstruction of water flow, the selected cross-sections are standardized to a uniform width of 12 m. The dimensions of cross-sections and the discretized meshes are rendered in Fig. 10.

Figure 11 demonstrates the geometry has significant effect on added mass and added damping. Specifically, the square shape exhibits the largest added mass compared to the other shapes, while the rounded rectangle shape exhibits the largest added damping. The fundamental period $T_{wet,square} > T_{wet,rectangle} > T_{wet,ellipse} > T_{circular}$ can be visualized in Fig. 12, indicating that the square shape induced the most significant added mass while the circle induced the least added mass. The damping ratio $\zeta_{wet,rectangle} > \zeta_{wet,square} > \zeta_{wet,ellipse} > \zeta_{circular}$, indicating that the rounded rectangle generates the most amount of radiated waves and the circle generates the least amount of radiated waves in one oscillation period. In summary, the pier-water coupling interaction of the square and rounded rectangle is more pronounced concerning added mass

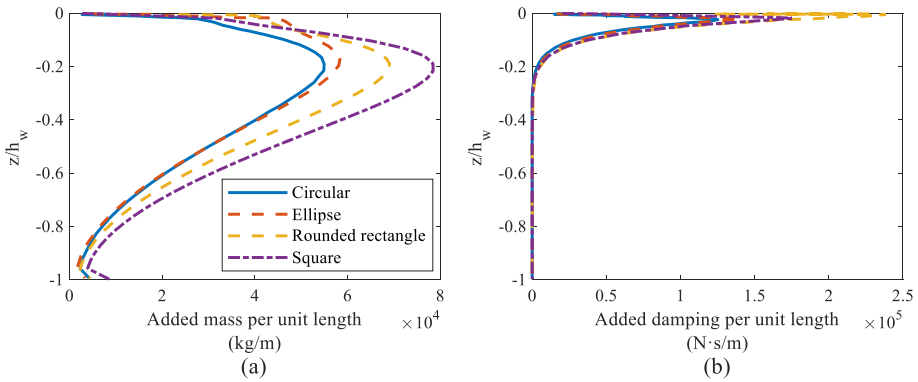

Fig. 11 Distribution of added mass and added damping along the pier height for different cross-sections

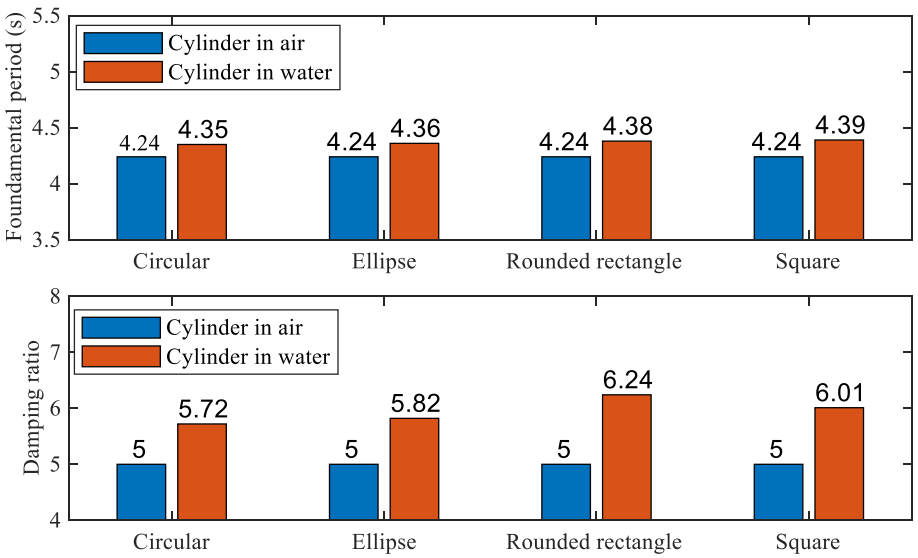

Fig. 12 Fundamental frequencies and damping ratios of bridge piers in air and water conditions for different cross-sections

and added damping, while the pier-water coupling interaction of the circular and elliptical form is close but not significant. The fundamental periods of the four cross-sections are found to be similar numerically, but the damping ratio differs significantly, indicating that the shape of the structural cross-section has a greater effect on the damping characteristics of the structure.

4 Conclusions

In this paper, a frequency domain boundary element method of pier-water coupling based on potential flow theory and modal superposition method was established. The general formulation of hydrodynamic added mass and added damping of elastic bridge piers with arbitrary cross-sectional shape was derived, and the period and damping ratio of the structure at pier-water coupling were obtained by an iterative scheme. The effectiveness of the model was verified using the benchmark test model from existing literature. To investigate

the effect of the pier-water coupling interaction on the added mass and added damping, a circular pier model was calculated using the developed method and the analytical formula without considering the structural elasticity. The effects of oscillating frequency and geometry of cross-section on added mass and added damping were investigated. The main findings were as follows:

(1) The developed method exhibits fine agreement with benchmark experimental results, confirming its effectiveness in simulating the fluid–structure coupling between elastic piers and water and accurately estimating the hydrodynamic added mass and added damping.
(2) The surface waves significantly affect the damping characteristics of the structure. Compared to the analytical method that neglect the surface wave effects, the developed method is capable of calculating added damping caused by surface wave effects. Considering the added damping leads to a notable increase of 14.4% in the damping ratio of the structure. This indicates that the surface wave effects induced by radiation should not be neglected.
(3) The oscillating frequency of the structure has a significant impact on the hydrodynamic added mass and added damping, especially near the water surface. This indicates that the surface wave effects induced by radiation primarily concentrate on the surface. The total added mass reaches its maximum value at a vibration frequency of 0.1 Hz, while the maximum value of the total added damping occurs at frequencies near the fundamental frequency.
(4) Geometry shows obvious impacts on the hydrodynamic added mass and added damping. The fundamental periods of different cross-sections show similarity, while the damping ratios exhibit significant variations, emphasizing the notable influence of the structural cross-sectional shape on the damping characteristics.

The structural characteristics and geometric shapes have an impact on the hydrodynamic added mass and added damping of elastic structures, so the conclusions drawn in this research are context-dependent and subject to variation based on the specific circumstances.

Acknowledgements
The authors would thank the colleagues from the Southwest Jiaotong University for the assistance and discussions.

Authors' contributions
Conceptualization, ZT; Formal analysis, ZT and YW; Investigation, YW; Supervision, ZT; Writing—original draft, ZT and YW; Writing – review & editing, ZT and YW. All authors have read and agreed to the published version of the manuscript.

Funding
This work was supported financially by the National Natural Science Foundation of China (Grant No. 52008349), Postdoctoral Science Foundation of China (Grant No. 2020M683356 and 2021T140573) and Natural Science Foundation of Sichuan Province (Grant No. 22NSFSC1163).

Availability of data and materials
All data present in the published article.

Declarations

Competing interests
The author(s) declared no potential conflicts of interest with respect to the research, authorship, and/or publication of this article.

Received: 3 August 2023 Accepted: 5 October 2023
Published online: 23 October 2023

References

Bai X (2018) Numerical simulation of wind wave current flows and dynamic performance investigation of bridge tower under wind-wave actions. Harbin Institute of Technology, Harbin
Chen X, Mei X (2016) Design of deepwater foundations of main ship channel cable-stayed bridge of Pingtan Straits Rail-cum-Road Bridge. Bridge Constr 46(3):86–91
Chen X, Chen Z, Xu G et al (2021) Review of wave forces on bridge decks with experimental and numerical methods. Adv Bridge Eng 2:21–24
Choi YR, Hong SY, Choi HS (2001) An analysis of second-order wave forces on floating bodies by using a higher-order boundary element method. Ocean Eng 28(1):117–138
Dong S, Jin F (2009) Analysis of self-vibration characteristics in Cangkou navigational bridge of Qingdao Bay Bridge. Highway 9:11–13
Guo A, Liu J, Chen W et al (2016) Experimental study on the dynamic responses of a freestanding bridge tower subjected to coupled actions of wind and wave loads. J Wind Eng Ind Aerodyn 159:36–47
Han RP (1996) A simple and accurate added mass model for hydrodynamic fluid—Structure interaction analysis. J Franklin Inst 333(6):929–945
Huang X, Li Z (2011) Influence of free surface wave and water compressibility on earthquake induced hydrodynamic pressure of bridge pier in deep water. J Tianjin Univ 44(4):319–323
Huang W, Yang Q, Xiao H (2009) CFD modeling of scale effects on turbulence flow and scour around bridge piers. Comput Fluids 38(5):1050–1058
Huang B, Zhu B, Cui S et al (2018) Experimental and numerical modelling of wave forces on coastal bridge superstructures with box girders Part I: Regular waves. Ocean Eng 149:53–77
Jiang H, Wang B, Bai X et al (2017) Simplified expression of hydrodynamic pressure on deepwater cylindrical bridge piers during earthquakes. J Bridg Eng 22(6):04017014
John F (1949) On the motion of floating bodies. I. Commun Pure Appl Math 2(1):13–57
John F (1950) On the motion of floating bodies II. Simple harmonic motions. Commun Pure Appl Math 3(1):45–101
Kim Y, Kring DC, Sclavounos PD (1997) Linear and nonlinear interactions of surface waves with bodies by a three-dimensional Rankine panel method. Appl Ocean Res 19(5–6):235–249
Kristiansen E, Egeland O (2003) Frequency-dependent added mass in models for controller design for wave motion damping. IFAC Proc Vol 36(21):67–72
Li Y, Chen Y (2011) The importance and technical difficulties of tunnel and islands for Hong Kong Zhuhai Macao Bridge Project. Eng Mech 28(A02):67–77
Li Q, Yang W (2013) An improved method of hydrodynamic pressure calculation for circular hollow piers in deep water under earthquake. Ocean Eng 72:241–56
Liaw C, Chopra A (1974) Dynamics of towers surrounded by water. Earthq Eng Struct Dyn 3(1):33–49
Liu Z (2019) Key construction techniques for Pingtan Straits Rail-cum-Road Bridge. Bridge Constr 49(5):1–8
Lu Z (2006) Key technologies for Hangzhou Bay Bridge. Chin Civil Eng J 39(6):78–82
Murray R, Rastegar J (2009) Novel two-stage piezoelectric-based ocean wave energy harvesters for moored or unmoored buoys. In: Active and Passive Smart Structures and Integrated Systems 2009, San Diego
Perić R, Abdel-Maksoud M (2016) Reliable damping of free-surface waves in numerical simulations. Ship Technol Res 63(1):1–13
Rahman M, Bhatta D (1993) Evaluation of added mass and damping coefficient of an oscillating circular cylinder. Appl Math Model 17(2):70–79
Romate J (1992) Absorbing boundary conditions for free surface waves. J Comput Phys 99(1):135–145
Shen J, Gou Y, Teng B (2012) Numerical simulation of the interaction between waves and floating elastic plate. Eng Mech 29(12):287–294
Teng B, Gou Y (2006) Hydroelastic analysis of very large floating structure in frequency domain. Eng Mech 23(S2):36–48
Teng B, Taylor RE (1995) New higher-order boundary element methods for wave diffraction/radiation. Appl Ocean Res 17(2):71–77
Ti Z, Zhang M, Li Y et al (2019) Numerical study on the stochastic response of a long-span sea-crossing bridge subjected to extreme nonlinear wave loads. Eng Struct 196:109287
Ti Z, Deng XW, Yang H (2020) Wake modeling of wind turbines using machine learning. Appl Energy 257:114025
Ti Z, Li Y, Qin S (2020b) Numerical approach of interaction between wave and flexible bridge pier with arbitrary cross section based on boundary element method. J Bridg Eng 25(11):04020095
Ti Z, Wei K, Li Y et al (2020c) Effect of wave spectral variability on stochastic response of a long-span bridge subjected to random waves during tropical cyclones. J Bridg Eng 25(1):04019131
Ti Z, Wang Y, Song Y (2022) Frequency-domain approach of aero-hydro-elastic response for offshore bottom-mounted slender structures under wind and wave. Ocean Eng 260:111795
Wang P, Mi Z, Du X (2018) Analytical solution and simplified formula for earthquake induced hydrodynamic pressure on elliptical hollow cylinders in water. Ocean Eng 148:149–60
Wang P, Zhao M, Du X et al (2018) Simplified evaluation of earthquake-induced hydrodynamic pressure on circular tapered cylinders surrounded by water. Ocean Eng 164:105–13
Wei K, Zhou C, Zhang M et al (2020) Review of the hydrodynamic challenges in the design of elevated pile cap foundations for sea-crossing bridges. Adv Bridge Eng 1(1):1–30
Westergaard HM (1933) Water pressures on dams during earthquakes. Trans Am Soc Civ Eng 98(2):418–433
Xing J, Price W, Pomfret M et al (1997) Natural vibration of a beam—water interaction system. J Sound Vib 199(3):491–512

Xu G, Cai C (2015) Wave forces on Biloxi Bay Bridge decks with inclinations under solitary waves. J Perform Constr Facil 29(6):04014150
Yang W, Li Q (2012) Natural vibration properties analysis of deep-water piers based on fluid structure interaction. Sichuan Build Sci 38(3):164–170
Yang W, Li S, Liu J et al (2021) Numerical study on breaking solitary wave force on box-girder bridge. Adv Bridge Eng 2(1):1–29
Yeung RW (1981) Added mass and damping of a vertical cylinder in finite-depth waters. Appl Ocean Res 3(3):119–133
Zhang J, Wei K, Qin S (2019) An efficient numerical model for hydrodynamic added mass of immersed column with arbitrary cross-section. Ocean Eng 187:106192
Zhao R, Zheng K, Wei X et al (2022) State-of-the-art and annual progress of bridge engineering in 2021. Adv Bridge Eng 3(1):1–71

Publisher's Note